Solid Earth Discuss., 6, 1155–1190, 2014
www.solid-earth-discuss.net/6/1155/2014/
doi:10.5194/sed-6-1155-2014

Solid Earth
Discussions
Open Access

Evaluating the importance of surface soil contributions to reservoir sediment in alpine environments: a combined modelling and fingerprinting approach in the Posets-Maladeta Natural Park

L. Palazón[1], **L. Gaspar**[2], **B. Latorre**[1], **W. Blake**[2], **and A. Navas**[1]

[1]Department of Soil and Water, Estación Experimental de Aula Dei (EEAD-CSIC), Avda, Montañana 1005, 50059, Zaragoza, Spain
[2]School of Geography, Earth and Environmental Sciences, Plymouth University, Plymouth, Devon, PL4 8AA, UK

Received: 1 April 2014 – Accepted: 2 April 2014 – Published: 7 May 2014

Correspondence to: L. Palazón (lpalazon@eead.csic.es)

Published by Copernicus Publications on behalf of the European Geosciences Union.

Title Page
Abstract | Introduction
Conclusions | References
Tables | Figures
◀| | |▶
◀ | ▶
Back | Close
Full Screen / Esc
Printer-friendly Version
Interactive Discussion

Abstract

Soil in alpine environments plays a key role in the development of ecosystem. Identify, maintain and preserve its resources, as well as recognize processes that would affect them are important and of practical interest. Environmental concerns about these fragile systems which are threatened by the human pressure and climatic change have stressed the need to gather information in soil erosion processes. As most mountain alpine environment the Benasque catchment is characterized by temperatures below freezing that can last from November to April, strong rainfall events and rugged topography. Indirect studies, such as combined model approaches, could be an alternative to evaluate soil erosion on these areas. In this study the complementary tools of Soil and Water Assessment Tool (SWAT) and fingerprinting procedure were used to assess an initial approach on soil erosion processes which take place in the area of the Posets-Maladeta National Park (Central Spanish Pyrenees). Soil erosion rates and sediment contribution of potential sediment sources (Kastanozem/Phaeozem; Fluvisol; Cambisol and channel bed sediments) were assessed. SWAT model identified Cambisols as the main source of sediment of the Benasque catchment with the highest specific sediment yields and Phaeozems and Fluvisols were identified as the lowest sediment contributors. Spring and winter performed the highest and lowest specific sediment yield, respectively. Fingerprinting procedure identified channel bed sediment and Fluvisols as the main sediment sources indicating the main influence of connectivity. The combined approach enabled us to better understand soil erosion processes in the Benasque alpine catchment.

1 Introduction

Alpine soil performs important ecological functions that are related to the quality and quantity of water resources, the storage of carbon, the risks of floods, the maintenance and character of biodiversity and the value of landscapes as habitats. Mountain soils suffer from intrinsic vulnerability to natural stresses such as extreme rainfall (Giannecchini et al., 2007; Meusburger and Alewell, 2008) and changes in precipitation (Stanchi et al., 2013). Soils are themselves a natural resource and their protection is vital for the proper and sustainable functioning of the alpine environment.

Mountain systems all over the world are unique in their ecology and diversity (Alewell et al., 2008). However, the extreme topography and climate, like in the Benasque alpine catchment (Spain) which is the focus of this study, result in high instability, fragility and sensitivity for these ecosystems (Gellrich and Zimmermann, 2007). Simultaneously, human society has exploited to maximum most mountain environments (Lasanta et al., 2006) which are experiencing serious degradation since the Middle Ages (Höchtl et al., 2005). Economic, societal and environmental changes are often an immediate threat to mountain systems and careful planning is needed (Alewell et al., 2008). Thus, methods to describe and predict ecosystem stability in mountain systems are urgently needed (Garcia-Ruiz et al., 1996). One inherent parameter of ecological stability is the status of soils in the ecosystems which affects mountain ecosystem like slope stability, water budgets (drinking water reservoirs as well as flood prevention), vegetation productivity, ecosystem biodiversity and nutrient production.

Although alpine soils generally have high density vegetation covers, they are vulnerable to soil erosion because of steep slopes and extreme climatic events. Vegetation cover is an important parameter with respect to soil erosion in mountain soils because protects soil by reducing water runoff and dampening the kinetic energy of rain drops, increasing water infiltration into the soil matrix and by sheltering and stabilizing the terrain by roots (Schindler Wildhaber et al., 2012). Changes of land use can modify the water balance in certain mountain areas with negative impacts on the lowlands, which support higher density of population. Depending on region and altitude, the projection of further warming will be shortened the duration of snow cover by up to 100 days with earlier snowmelt in spring (Beniston, 2006; Horton et al., 2006; Jasper et al., 2004). In Europe, a rising snowline, intensified precipitation during the winter and strong leaching effects with no or sparse vegetation cover in late fall and early spring will result in an increase of erosion (Fuhrer et al., 2006). Nevertheless, increased erosion is also likely in the alpine environment where extreme droughts will be followed by rain events of increased intensity (Brunetti et al., 2006; Schmidli and Frei, 2005) or rapid snowmelt in late spring will be overlapped with intense rain events producing large catastrophic floods, as observed on 18 January 2013 in the Benasque catchment.

Sediment production and yields to the hydrological network in alpine environments are conditioned by the characteristics of high mountain climate especially with the presence of the snow cover periods and its related snowmelt. During the winter one of the processes affecting soil aggregates stability is freezing and thawing cycles providing small soil aggregates which would be easily exported by the early spring snowmelt. This has a great influence on the spring soil's erodibility. In addition, these regions are mostly characterized by rugged topography and large precipitation, that favored quickly and substantial runoff.

In the near future, the combined effects of global climate and land use change might significantly increase soil degradation (Beniston, 2006; Fuhrer et al., 2006). Suitable methods to describe and predict soil degradation in mountain areas with low accessibility, steep topography and extreme climate are urgently needed for suitable planning processes in Alpine regions under global change regime (Alewell et al., 2008). Low accessibility characteristics of these regions make that the indirect methods, such as models or numerical approaches, became useful and economical tools to conduct studies on soil degradation.

The Soil and Water Assessment Tool (SWAT) (Arnold et al., 1998) is a hydro-sedimentary model that was developed to predict the effects of different management practices on water quality, sediment yield and pollution loading in watersheds. SWAT has been widely implemented to perform hydrological simulations to estimate streamflow timing and volumes from mountainous catchments worldwide (e.g. Gikas et al., 2006; Zhang et al., 2008; Yu et al., 2011; Rahman et al., 2013). However, there have been few studies that evaluate sediment production in alpine mountain catchments (Abbaspour et al., 2007; Rostamian et al., 2008; Flynn and Van Liew, 2011).

Viewed in simple terms, sediment source fingerprinting applied to catchment systems aims to provide information on the source of the sediment transported by a river (Walling, 2013). The fingerprinting procedure employs statistical testing of a range of source material tracer properties to select a subset that discriminate sources (Collins and Walling, 2002). Sediment fingerprinting approaches offer potential to quantify the contribution of different sediment sources, evaluate catchment erosion dynamics and support the development of management plans to tackle the reservoir siltation problems. In the last 30 years, sediment source fingerprinting investigations have expanded greatly related to a growing need for information on sediment source and to technological advances which facilitate such work (Walling, 2013). However, source fingerprinting techniques continue to be most widely applied in agricultural catchments (e.g. Owens et al., 2000; Collins et al., 2010; Martínez-Carreras et al., 2010b; Blake et al., 2012).

The Benasque alpine catchment in Posets-Maladeta Natural Park, located in the Central Spanish Pyrenees, is surrounded by the highest peaks (> 3000 m a.s.l.) of the Pyrenean Range. Soil loss due to water erosion represents an increasing threat under conditions of climate change which affects precipitation regimes, frequency of extreme meteorological events, snow melt and vegetation as stated in the IPCC report (2007). This study constituted a preliminary approach to understand soil erosion processes in the Benasque alpine catchment. The aim of this study is to adopt a combined modelling and tracing approach for assessing soil erosion processes in alpine soils and for identifying sources of sediments. Specific objectives are: (1) to undertake spatial and temporal modeling with SWAT to identify soils which generate sediment and yield into streams that inflow into two small reservoirs; (2) to use composite fingerprinting properties to identify the principal sources of sediment delivered to the reservoirs.

2 Study area

The Benasque catchment is located within the Posets-Maladeta Natural Park (Central Spanish Pyrenees). The Natural Park, created in 1994, is an autonomic legisla-

Title Page
Abstract Introduction
Conclusions References
Tables Figures
◀◀ ▶▶
◀ ▶
Back Close
Full Screen / Esc
Printer-friendly Version
Interactive Discussion

tive figure engaged in the conservation of natural species and values. It has a great biological diversity typical of high mountain bioclimatic zones with endemic species or endangered species and in the future could be included in the National Park network. The glacial shaped valley, the moraines and glacial lakes and, in the same way, the karstic phenomenon in its headwater are of great interest. The remnant Aneto-Maladeta glacial system is located in the northernmost part of the catchment.

The catchment is situated in the Axial Pyrenees Structural Unit composed of Paleozoic rocks (quartzites, limestone, and slates) and granodiorites with a very complex tectonic organization. The mean elevation of the catchment is 2213 m a.s.l. and ranges from 1039 m a.s.l. at the outlet to 3404 m a.s.l. (Aneto Peak). The climate is defined as mountain type, wet and cold, with both Atlantic and Mediterranean influences (García-Ruiz et al., 1985). The village of Benasque at 1138 m a.s.l., receives an average annual precipitation of 1182 mm which further increases to more than 2500 mm on the highest divides (García-Ruiz et al., 2001). Above 1000 m a.s.l., the average annual temperature is lower than 10 °C and at 2000 m the mean temperature is around 5 °C (Puigdefábregas and Creus, 1973). Thus, between November and April, the 0 °C isotherm is around 1600–1700 m a.s.l. (García-Ruiz et al., 2001) representing that more than 85 % of the catchment is above this isotherm (Fig. 1). The hydrologic regime of the area is transitional nivo-pluvial with clear nival trends tempered by pluvial influences (López-Moreno et al., 2002). The study catchment includes two reservoirs Linsoles and Paso Nuevo (Fig. 1), both with a storage capacity of 3 hm^3, regulate 118 and 283 km^2 of the Ésera headwater, respectively, with an impounded runoff index (IR) of 0.016 and 0.022 each. Based on their IR index and using the equation developed by Heinemann (1981) for small reservoirs, Linsoles and Paso Nuevo have a 45 and 60 % of sediment trap efficiency, respectively. The hillslopes derived sediment loads transported through the reservoirs and the fluvial network are effectively exported out of the catchment. The river has clean blocky alluvial deposits and rocky embedded channels.

A well developed karst system is located in the northern area of the catchment (Fig. 1) and the discharge of the upper part of the Ésera River flows underground through the Jueu karst system to the upper Garonne River (Aran Valley, Spain).

Rock outcrops cover more than 25 % of the catchment (Table 1). The cultivation areas, range grasses and vegetable gardens, are very small (3 %) and limited to the valley floors. The pine forest of *Pinus sylvestris* is the most important between 1200 and 1700 m a.s.l., alternating with *Abies alba* and even small formations of *Fagus sylvatica* in shady places. However, above 1700 m many forests have been removed to facilitate the extension of pasture (García-Ruiz and Del Barrio, 1990). Above 2500 m bare rocks with sparse plants increasingly dominate the landscape.

The soils of the catchment are stony, shallow and alkaline, overlying fractured bedrock with textures from loam to sandy loam. Because the Benasque catchment was deglaciated at the beginning of the Holocene the soils of the catchment are young and strongly influenced by a periglacial environment. On steep slopes, where Leptosols (with rendzic Leptosols) and lithic Kastanozems are developed, soils are shallow and regularly truncated. More developed soils, as Cambisols, Phaeozems are found in the catchment bottoms and Fluvisols cover the valley floors (Fig. 2 and Table 1).

3 Material and methods

3.1 The SWAT model

SWAT, the Soil and Water Assessment Tool, is a physically-based, semi-distributed, agro-hydrological model that operates on a daily time step (as a minimum) at catchment scale (Arnold et al., 1998). The model is capable of continuous hydrological simulation in large complex catchments with varying weather, soils and management conditions. Major model components include weather, hydrology, soil temperature and properties, plant growth, nutrients, pesticides, bacteria and pathogens, and land management.

Theory and details of different processes integrated in SWAT model are available online in SWAT documentation (http://swatmodel.tamu.edu/).

SWAT can analyze catchments by discretising into sub-basins, which are then further subdivided into hydrological response units (HRUs). The sediment from sheet erosion for each HRU is calculated using the Modified Universal Soil Loss Equation (MUSLE; Williams and Berndt, 1977). Erosion and sediment delivery are estimated as a function runoff energy factor and physical factors such as soil erodibility, slope steepness and cover factor, which correspond to flow volume within the channel on a given day. Water redistribution in the HRUs is affected by soil temperature. If temperature in a particular soil layer is $\leq 0\,^{\circ}$C, no redistribution is allowed from that layer. Moreover, the erosive power of rainfall and runoff will be less when snow cover is present than when there is no snow cover. The computed loads are then routed through the channel network based on a simplified version of the method of Bagnold (1977), where sediment deposition or erosion is determined based on the unique sediment transport capacity of the individual routing reach and by the upstream continuum of sediment from other subcatchment and channel reaches (Neitsch et al., 2010).

3.1.1 SWAT inputs

The HRUs are defined by distinctive combinations of categorized land covers, soil types, and slope. Compiling the input data needed to run the model required considerable research, as well as documenting and adapting the available information, since there were few or no tabulated data to characterize the catchment. For this approach, input data for the Barasona catchment, a larger SWAT project in which the Benasque catchment is the headwater was used (Palazón and Navas, 2014).

The topographic information was based on a digital elevation model (DEM) obtained from the National Geographic Institute (IGN, 2011) with a 25 m grid cell spatial resolution. Given the large slope variations in the watershed, five categories of slope (0–20 %, 20–40 %, 40–60 %, 60–75 % and > 75 %) were defined and derived to the DEM to characterize the variety of the different surfaces (Fig. 2).

Title Page
Abstract Introduction
Conclusions References
Tables Figures
◀| |▶
◀ ▶
Back Close
Full Screen / Esc
Printer-friendly Version
Interactive Discussion

The Digital Soil Map of Aragón at a scale of 1 : 500 000 (Soil Map of Aragón, MACHÍN, unpublished data, 2000) was used to define 5 soil types across the Linsoles catchment (Fig. 2). A user soil database was developed with the required information on the soil types and incorporated within the ArcSWAT soil database to characterize each soil type. The soil parameters were defined based on field samples, literature, mathematical model and field observations for the catchment. The USLE soil erodibility K-factor was calculated according to a general equation developed by Williams et al. (1975) recommended by the input/output documentation of the model (Neitsch et al., 2010).

The land cover map was extracted from the European Project Corine Land Cover map (2000) with a resolution of 100 m. The 14 categories identified in the catchment were evaluated to assign an equivalent class in the SWAT2009 database (Fig. 2). Finally, the overlaid spatial input data lead to the definition of 853 HRUs within ArcSWAT.

Climate inputs available and used in this SWAT project were daily minimum and maximum temperature and rainfall data. They were based on measured data within or close to the region (Fig. 1). Data sources were obtained from the Governmental Meteorological Agency (AEMET, Agencia Estatal de Meteorología).

3.1.2 Catchment parameterizations in SWAT

The discharge of flow by the karst system outside the catchment was simulating by forcing SWAT to drain all of the simulated runoff of the headwater subcatchment limited by the Renclusa swallow hole (Fig. 1; Palazón and Navas, 2013). The drainage area limited by the karst system (30 km^2) was excluded for the soil sediment production evaluation.

Reservoir parameterizations for Linsoles and Paso Nuevo reservoirs in SWAT were based on their technical characteristics (reservoir area, principal and emergency spillways volume) and simulated controlled outflow-target release. The equilibrium sediment concentration of 0.058 and 0.065 g L^{-1} for the small reservoirs Linsoles and Paso

Nuevo were manually calibrated to produce simulated trap efficiency of 45 and 60 %, respectively.

To account for climate elevation gradients of the Linsoles catchment, 10 homogeneous elevation bands and their estimated altitudinal gradients on precipitation and temperature for the study area were defined in each subcatchment. The altitudinal temperature gradient (TLAPS: temperature lapse rate in SWAT) was set at $-5\,^{\circ}\mathrm{C\,km^{-1}}$ (García-Ruiz et al., 2001) and the altitudinal precipitation gradient (PLAPS: precipitation lapse rate in SWAT) was set at $1000\,\mathrm{mm\,km^{-1}}$ for most of the watershed and was accordingly decreased by subwatershed in relation to the number of elevation bands above 2000 m a.s.l. It is widely documented that the precipitation altitudinal gradient decreases to almost half in the study area at heights above 2000 m. Finally, the PLAPS for the subwatersheds range from 550 to $1000\,\mathrm{mm\,km^{-1}}$.

Calibration of SWAT was necessary as the model is composed of a large number of parameters that define various catchment characteristics and processes. As the headwater of the Barasona catchment is the Benasque catchment, the calibrated parameters for the Barasona catchment, as validated for flow and sediment in a previous work (Palazón and Navas, 2014), were used in this study. As no temperature index method or equivalent snow data of the study area were available, defining the snowfall-snowmelt processes in SWAT for this mountainous watershed was an important part of the calibration. The default SWAT values of the snow routine parameters were manually modified in the way to obtain resultant snowfall and snowmelt values in good agreement with the snow retention and snowmelt streamflow observed in the region.

The calibrated scenario was conducted over a period of 4 years (2003–2006) preceded by a three-year model “warm-up” initialization period. The model period was selected to include a variety of climatic and hydrological conditions.

3.2 Sediment fingerprinting procedure

The standard sediment source fingerprinting procedure is based on (i) statistical analysis of difference to identify a subset of tracer properties that discriminate the sediment sources followed by (ii) the use of multivariate mixing models comprised of a set of linear equations for each selected tracer property to estimate the proportional contributions from each source (Yu and Oldfield, 1989; Collins et al., 1997; Walden et al., 1997; Blake et al., 2012; Smith and Blake, 2014). Uncertainty in source estimates is quantified using a Monte Carlo routine that repeatedly solves the mixing model using random samples drawn from probability distributions derived for source groups (Franks and Rowan, 2000).

3.2.1 Sediment and soil sampling

To characterize the signatures of potential sediment source materials, representative sites were selected in areas where there was high potential sediment yield connectivity from hillslope to channel with easy access. A total of 50 individual samples were collected including 32 soil samples and 18 channel bed sediments. Twelve samples of sediment deposited in the reservoirs, were collected to permit comparison of reservoir silt to sources. These comprised 6 individual samples from each of the two small headwaters reservoirs. Sampling was done by using a cylindrical core 5 cm long and 6 cm of diameter.

Composite soil samples were generated from undisturbed soils by four individual samples collected from 0 to 5 cm depth and combined in the field to form a single composite sample. The depth of sampling interval was selected because stoniness and high surface soil roughness in the study soils. Of the soil samples, 2 were composite samples from Cambisols, 3 from Fluvisols and 3 composite samples from Kastanozems and Phaeozems. Leptosols were not sampled because in addition of being very poorly developed and shallow soils, they occupy areas of very high slope with more than its 50 % extend in areas with more than 60 % of slope, which was difficult to access. It was decided to concentrate efforts for this preliminary research on the better developed soils of the catchment which were connected to the channel.

Exposed channel bed fine sediments were sampled as they represent material delivered from the upstream catchment, an integrated source area. A field survey was carried out to select the sampling sites for collecting exposed channel bed samples in the four main tributaries to the Ésera River. In each tributary two locations were established upstream close to the headwater and downstream at a minimum distance of 3 km to the inflow in the Ésera River. From the eight selected locations, only three of them had fine exposed channel bed materials for sampling. In each site a total of six samples were collected along transects of 100 m long and mixed up to prepare 3 composite samples representative of the sediment deposited and being transported in the channel reach. In general, the Ésera River flows through blocky or rocky channels. Channel banks are not developed or they are very local with maximum river incisions of 10–15 cm in the soils of the valley bottoms and, therefore, they were not sampled.

Sediments from the Paso Nuevo and Linsoles reservoirs were sampled at the accessible areas of the reservoir delta. In each reservoir, a composite sediment sample was prepared in the field with a minimum of 6 fine sediment samples of exposed reservoir deposits. All samples were initially oven-dry at 35 °C, gently disaggregated and sieved to < 63 µm to isolate a standardised grain size fraction.

3.2.2 Laboratory analyses

Analysis of the grain size was performed using laser diffraction particle size analyser. Prior to the analysis, organic matter was eliminated with an H_2O_2 (10 %) digest heated to 80 °C. Samples were disaggregated with sodium hexametaphosphate (40 %), stirred for 2 h and dispersed with ultrasound for a few minutes. The contents of soil organic carbon, both active and stable carbon fractions, were analysed by the dry combustion method using a LECO *RC-612* multiphase carbon analyser designed to differentiate forms of carbon by oxidation temperature (LECO, 1996) in a sub-sample of the < 63 µm fraction that had been ground to a very fine powder with a mortar and pestle. Mass specific magnetic susceptibility (χ) was measured using a Bartington Instruments dual-frequency MS2B sensor that operates with an alternating current producing an alternating magnetic field at 80 $\mathrm{A\,m^{-1}}$ (Bartington Instruments Ltd. 2000). The MS2B sensor can be operated at two different frequencies, at low frequency 0.47 kHz (LF) and at high frequency 4.70 kHz (HF). The < 63 µm fraction of the samples were placed in 10 mL sample containers and χ was measured at each frequency and the frequency dependence of susceptibility (χ_{FD}) was obtained. Mass specific magnetic susceptibility at low (χ_{LF}) and high (χ_{HF}) frequency measurements was expressed as $10^{-8}\,m^3\,kg^{-1}$. In this study three measures of mass specific magnetic susceptibility were taken from each sample and the average was reported. The χ_{FD} was the percentage of difference between χ_{LF} and χ_{HF}, therefore the χ_{HF} was considered redundant and had not been included in the statistical analysis of the fingerprinting procedure.

The analysis of the total elemental composition was carried out after total acid digestion with HF (48 %) in a microwave oven (Navas and Machín, 2002). Samples were analysed for the following 28 elements: Li, K, Na (alkaline), Be, Mg, Ca, Sr (light metals), Cr, Cu, Mn, Fe, Al, Zn, Ni, Co, Cd, Tl, Bi, V, Ti and Pb (heavy metals), B, Sb, As (metalloids), and P, S, Mo and Se. Analyses were performed by atomic emission spectrometry using inductively coupled plasma ICP. Concentrations, obtained after three measurements per element, are expressed in $mg\,kg^{-1}$. Those elements returning measurements below the detection limit (Co, Cd and Se) have been excluded in the analysis. P was also excluded on the basis of the risk of non-conservative behavior during downstream transport (Granger et al., 2007).

The methods used in the analysis of radionuclides are described in detail elsewhere (Navas et al., 2005a, b). Radionuclide activity concentrations in the soil samples were measured using a Canberra high resolution, low background, hyperpure germanium coaxial gamma detector coupled to an amplifier and multichannel analyser. The detector had a relative efficiency of 50 % and a resolution of 1.9 keV (shielded to reduce background), and was calibrated using standard samples that had the same geometry as the measured samples. Subsamples of 50 g were loaded into plastic containers. Count times over 24 h provided an analytical precision of about ±3–10 % at the 95 % level of confidence. Activities were expressed as $Bq\,kg^{-1}$ dry soil.

Gamma emissions of ^{238}U, ^{226}Ra, ^{232}Th, ^{40}K, ^{210}Pb, and ^{137}Cs (in $Bq\,kg^{-1}$ air-dry soil) were measured in the bulk soil samples. Considering the appropriate corrections for laboratory background, ^{238}U was determined from the 63-keV line of ^{234}Th, the activity of ^{226}Ra was determined from the 352-keV line of ^{214}Pb (Van Cleef, 1994); ^{210}Pb activity was determined from the 47 keV photopeak, ^{40}K from the 1461 keV photopeak; ^{232}Th was estimated using the 911-keV photopeak of ^{228}Ac, and ^{137}Cs activity was determined from the 661.6 keV photopeak. The ^{210}Pb (half-life = 22.26 yr) is integrated by the "in situ"-produced fraction from the decay of ^{226}Ra (Appleby and Oldfield, 1992) and the upward diffusion of ^{222}Rn in the atmosphere, which is the source of $^{210}\text{Pb}_{\text{ex}}$. Spectrometric measurements were performed a month after the samples were sealed, which ensured a secular equilibrium between ^{222}Rn and ^{226}Ra. The $^{210}\text{Pb}_{\text{ex}}$ activities were estimated from the difference between the total ^{210}Pb activity and the ^{226}Ra activity.

3.2.3 Statistical analysis for source discrimination

Examination of the range of source and sediment tracer concentrations is an important assessment of the conservative behavior of each tracer property (Martínez-Carreras, 2010b; Wilkinson et al., 2012; Smith and Blake, 2014). In this study, the range in source tracer concentrations was compared to the range in sediment concentrations for each reservoir, with those tracer properties falling outside the range in source values were removed from subsequent analysis.

Statistical analysis of remaining tracer properties first involves using the nonparametric Kruskal–Wallis *H* test to identify and eliminate redundant tracer properties that do not exhibit a significant difference between source categories (Collins and Walling, 2002). It tests the null hypothesis that tracer properties exhibit no significant differences between source categories. Larger differences between categories generated greater *H* test statistic. A stepwise Discriminant Function Analysis (DFA) was used to test the ability of the tracer properties passing the Kruskal–Wallis *H* test to confirm the existence of inter-category contrast. The DFA select an optimum composite fingerprint that comprises the minimum number of tracer properties that provide the greatest discrim-

Title Page
Abstract Introduction
Conclusions References
Tables Figures
◂◂ ▸▸
◂ ▸
Back Close
Full Screen / Esc
Printer-friendly Version
Interactive Discussion

ination between the analyzed source materials based on the minimisation of Wilks' lambda. The lambda value approaches zero as the variability within source categories is reduced relative to the variability between categories based on the entry or removal of tracer properties from the analysis. The results of the DFA are used to examine the proportion of samples accurately classified into the correct source groups.

3.2.4 Multivariate mixing model

The relative contribution of each potential sediment source was assessed by Monte Carlo mixing model using a new data processing methodology to obtain proportional source contributions for the reservoir sediment samples. Similar to other approaches (e.g. Evrard et al., 2011), the model seeks to solve the system of linear equations by means of mass balance equations represented by:

$$\sum_{j=1}^{m} a_{i,j} \cdot x_j = b_i$$

While satisfying the following constraints:

$$\sum_{j=1}^{m} x_j = 1$$

$$0 \le x_j \le 1$$

where, b_i is the value of tracer property i ($i = 1$ to n) in the reservoir sediment sample, $a_{i,j}$ is the mean concentration of tracer property i in source type j ($j = 1$ to m), x_j is the unknown relative weighting contribution of source type j to the suspended sediment sample, m is the number of potential source types, and n is the number of tracer properties selected by the DFA.

The new approach adopted here used a Combinatorial Principals method which was solved by a Monte Carlo sampling routine to identify the most probable solution with associated uncertainty based on source variability. The model was written in C programming language and designed to deliver a user-defined best number possible solutions and iterations. The unique solution from the generated iterations (p = random positive numbers) for each sediment sample was characterized by the mean weighting source contribution, the standard deviation of the user-defined solutions and their lower goodness of fit (GOF) index (Motha et al., 2003) defined by:

$$\mathrm{GOF} = 1 - \frac{1}{p} \times \left(\sum_{i=1}^{n} \frac{\left| b_i - \sum_{j=1}^{m} x_j \bar{a}_{i,j} \right|}{b_i} \right)$$

This method is argued to guarantee a similar set of representative solutions in all unmixing cases based on likelihood of occurrence. Source samples for the different potential sediment sources of the drainage basin were compared with samples from the reservoirs using the optimum composite fingerprint defined by the DFA. In this case, the model was configured to select the 10 best results obtained from 10^6 generated random positively solutions using multiple start values for each sediment reservoir sample.

4 Results

4.1 Soil specific sediment yields by SWAT model

The temporal distribution of the simulated sediment yields for the Linsoles gauge station agreed with the simulated streamflows (Fig. 3). The average simulated sediment yield that inflow to Paso Nuevo and Linsoles reservoirs were 12 543 and 26 145 t year^{-1}, respectively. The simulated streamflow of the study period (2003–2006) showed the characteristics of the nivo-pluvial regime. The monthly inflow discharge at the Linsoles reservoir performed a satisfactory Nash–Sutcliffe coefficient of 0.62 (Nash and Sutcliffe, 1970).

Application of the SWAT model for the Benasque catchment enabled investigating the sediment yields generated from the different soil types and their temporal dynamics. The soil specific sediment yield ($\mathrm{t\,ha^{-1}\,year^{-1}}$) presented substantial differences in productions (Table 2). The greatest modelled specific sediment yield was produced from Cambisols, followed by Kastanozems and then Leptosols. The specific sediment yield from Cambisols was three times greater than from Kastanozems thus suggesting that these are the main soil source of sediments to the Ésera River. The lowest sediment production was from Fluvisols and Phaeozems.

In general, the snowmelt together with the spring season performed the highest modelled soil specific sediment yield followed by the autumn season whereas the lowest soil specific sediment yields was performed in summer and winter (Fig. 4). Cambisols, Kastanozems, Leptosols and Phaeozems yielded the highest specific sediment yield in spring and autumn whereas the lowest was during summer and winter. However, Fluvisols showed a different pattern performing its lowest specific sediment yield in spring.

4.2 Soil and sediment source contributions

In this study, two sediment source options were evaluated. The first option involved the sediment contributions from soil and channel bed sediment sources and the second one considered only the soils as sediment sources. Proportional source contributions to sediment reservoir samples were estimated for the Paso Nuevo and Linsoles reservoirs for the two selected options.

To identify main sources of sediments firstly the conservative behaviour of the properties (Table 3) for the selection of the optimum fingerprint was considered for both options. $^{210}\mathrm{Pb_{ex}}$ was excluded as a sediment source fingerprint because sediments deposited in the reservoir will contain both $^{210}\mathrm{Pb_{ex}}$ incorporated into the sediment by direct fallout to the reservoir and that associated with sediment eroded from the upstream catchment. SOC and grain size fractions are considered non conservative properties and therefore, they were also excluded from the analyses (Koiter et al., 2013).

For the first option, the comparison of the range in tracer properties concentrations for source and sediment samples resulted in the exclusion of Al, B, Mg, and Tl for the statistical analysis. Kruskal–Wallis *H* test resulted in the selection of ^{137}Cs, ^{238}U, S and Zn as potential properties to discriminate between sediment sources (significance $p < 0.05$). The DFA selected ^{137}Cs, ^{238}U and Zn as the optimum source fingerprinting for the catchment based on the tracer properties passing the previous steps. The optimum fingerprint comprises the minimum number of properties that provide the greatest discrimination between sources.

For the catchment, apparently good source discrimination was achieved based on Wilks' lambdas of 0.017 and the percentage of correctly classified sources was 100 % (Table 4). Source unmixing model used all tracer properties that were selected by the DFA and the model goodness of fit (GOF) was calculated for each sediment reservoir sample and the standard deviation for each source apportionment. The outputs of the mixing model appeared to be stable, all outputs being very close and systematically within a range of < 8 % to their mean value. Mean proportional contributions from Kastanozems/Phaeozems, Cambisols, Fluvisols and channel bed sources varied between reservoir samples (Table 5). The preliminary results using this new data processing methodology for samples collected in the reservoirs allowed us to identify Fluvisol and channel bed sediments as main potential sources of sediments to the reservoirs. Paso Nuevo and Linsoles sediment samples had GOF > 80 %. The Paso Nuevo reservoir sample had the lowest mean GOF and the largest predicted uncertainty. Kastanozems/Phaeozems sources were estimated to contribute an apparently negligible amount of sediment to both reservoirs. For the Paso Nuevo reservoir, Fluvisols were identified as the main source contributing five times more than Cambisols. However, for the Paso Nuevo reservoir channel bed sediment constituted the principal source with apportionments 10 times greater than Cambisols.

Considering channel bed sediment source as secondary source the second option evaluated only soil sources. In addition from the first option, the range of the tracer properties for the second option of sources resulted in the exclusion of ^{137}Cs, ^{226}Ra, Bi, Cu, Mo, S and Ti. The Kruskal–Wallis *H* test resulted in the null identification of tracer properties to discriminate between sediment sources (significance $p < 0.05$). The DFA selected K, Sr, ^{238}U, Sb and LF as the optimum source fingerprinting for the catchment based on the tracer properties passing the first step. Based on Wilks' lambdas (Table 4) and the 100 % percentage of correctly classified sources apparently good source discrimination was achieved. For the second option the outputs of the mixing model appeared to be very stable, all outputs being very close and systematically within a range of < 1 % to their mean value. Mean proportional contributions from soil sources varied also between reservoir samples but both reservoir had GOF > 82 % (Table 5). Kastanozems/Phaeozems sources in this option apparently contributed for the Linsoles reservoir whereas null contribution resulted for the Paso Nuevo. For both reservoirs Fluvisols were identified as the main source contributing eight times more than the rest sources.

5 Discussions

SWAT model identified Cambisols as the main source of sediment of the Benasque catchment with the highest specific sediment yields and Phaeozems and Fluvisols were identified as the lowest sediment contributors. The greater stability of Phaeozems their vegetation cover mostly forested and location in areas with lowest slope ranges at the bottom of the catchment, were the reasons for the low simulated specific sediment yield. Fluvisols also occupy level surfaces and are covered by grass. Winter sediment production from Leptosols could be due to their steep slope and the location of the soils within a high precipitation gradient and under the 0 °C isotherm which means more rainfall. In addition of receiving relatively more rainfall than the other soils, runoff was especially higher in the wettest year of the period (2003).

The presence of snow cover restricted soil erosion. Soil temperature below 0 °C and snow cover limited sediment yields and streamflows in winter. The differences between observed and simulated hydrographs (Fig. 3) for the Linsoles gauge station show a general overestimation of the related autumn streamflows that might be due to limitations in the climate characterization for the highly variable climatic characteristics of the Benasque catchment. In addition, the simulated monthly discharge of the Paso Nuevo reservoir may contribute to amplify these differences.

Differences in discriminant tracer properties between assessed sources fingerprinting options were due to differences in tracer sources ranges that were most restricted in the second option for only soil sources. Moreover, the exclusion of the channel bed sediment as source for the second option limited the discriminant power of tracer properties because soil sources were less different, as Kruskal–Wallis *H* test resulted without significant difference in tracer properties between source categories. The highly dynamic fluvial systems existing in the catchment together with the location of the samples within the reservoirs might restrict representation in the fingerprinting procedure of the finer sediments that can be exported out of the reservoir or located at the inner parts of the reservoir in the delta dam.

Differences in soil and sediment apportionments between reservoir samples could be due to the characteristics in fluvial dynamics and soil underlaying the different upstream of their contributing areas (Table 1). Paso Nuevo reservoir has a higher fluvial dynamic with more steep slopes and greater percentage of Cambisols than Linsoles reservoir. In addition, Paso Nuevo subcatchment received greater precipitations because the altitudinal climatic gradients of the catchment. The channel bed sediment was included for the first option assessment as sediment source contributor. The short sediment residence time in the channels observed in the catchment with mostly clean blocky channel bed support the use of the channel bed sediment as source. Channel bed sediment source apportionment assessed with the first option for the Linsoles reservoir was greater than for the Paso Nuevo reservoir because of the higher number of tributaries present within the Linsoles reservoir subcatchment but it must also be borne in mind that these sediments represent a composite of the upstream material. By eliminating the channel bed sediment source the second fingerprinting option confirms that connectivity is a main control of sediment source contributions identifying the highest apportionments from Fluvisols in this evaluation.

Contributions from Cambisols for the sediment reservoir samples in both fingerprinting procedures could be considered concordant and point to Cambisols as one of the main soil sediment source being in SWAT the major source. However, great differences in Fluvisols contribution in the fingerprinting approaches and SWAT model outputs could be due to the difference in the temporal and spatial scale of the procedures. The temporal discrepancy requires further investigation e.g. through fingerprinting analysis of the temporal sequence within the sedimentary record of sediments from the middle of the reservoir. The spatial discrepancy was related to the resolution of SWAT soil inputs that could not reflect a detailed soil distribution extend and might not account all soil erosion processes. Fluvisols occupy the bottoms of the glacial shaped catchment and more than 85 % of their surfaces have slope range between 0–20 % in SWAT. The drainage of these relatively flat surfaces is done by small streams that concentrate runoff from the steep slopes. Therefore, the erodibility of Fluvisols could be undervalued by SWAT model.

The SWAT soil sediment productions assessment depended on the spatial and temporal distribution of large number of input data. However, the fingerprinting approach depended of the discriminatory power of the analyzed properties from the selected sources. In general, for both procedures sediment land cover sources were the most evaluated sediment sources in the literature (e.g. Martinez-Carreras, 2010b; Smith and Blake, 2014; Collins et al., 2013), though, discrimination of the soil sources with the fingerprinting procedure was possible for the alpine Benasque catchment because of its distinctive soil characteristics.

6 Conclusion

The use of the SWAT model permitted to identify Cambisols as the main soil source of sediment and the spring season as the highest sediment productions season for the

Benasque catchment. The fingerprinting approach point to Fluvisols and channel bed sediments as main contributing sources to the sediment accumulated in the reservoirs supporting the main influence of connectivity.

The combined use of SWAT model and sediment fingerprinting in the study of soil erosion processes for the alpine Benasque catchment provided information from two temporal views, continuous and instantaneous. The SWAT model provided information, quantification and identification of the sediment production and its temporal dynamic evolution of the individual selected soil sediment sources based on factors such as runoff energy, soil erodibility, slope steepness and cover factor (MUSLE), which correspond to flow volume within the channel on a given day. Whereas, the fingerprinting approach provided information about "instantaneous" sediment source contributions to the assessed sediments from the reservoirs, a "snapshot" of the sources recently deposited. Although temporal results from the assessment procedures were different, they could be considered complementary. However, further research is needed to ascertain if fingerprinting procedures could be used to verify model performance.

These initial findings demonstrate that a combined fingerprinting approach and modelling approach can offer insights in the temporal patterns of sediment delivery to reservoirs. The work undertaken here in an alpine Spanish Pyrenees catchment, will enable us to better understand the soil erosion processes in alpine environments.

Acknowledgements. This research was funded by the EROMED project (CGL2011-25486).

References

Abbaspour, K. C., Yang, J., Maximov, I., Siber, R., Bogner, K., Mieleitner, J., Zobrist, J., and Srinivasan, R.: Modelling hydrology and water quality in the pre-Alpine/Alpine Thur watershed using SWAT, J. Hydrol., 333, 413–430, 2007.

Alewell, C., Meusburger, K., Brodbeck, M., and Bänninger, D.: Methods to describe and predict soil erosion in mountain regions, Landscape Urban Plan., 88, 46–53, 2008.

Appleby, P. G. and Oldfield, F.: Application of lead-210 to sedimentation studies, in: Uranium-Series Disequilibrium: Application to Earth, Marine and Environmental Sciences, edited by: Ivanovich, M., and Harman, R. S., Clarendon Press, Oxford, UK, 731–738, 1992.

Arnold, J. G., Srinivasan, R., Muttiah, R. S., and Williams, J. R.: Large Area Hydrologic Modelling and Assessment Part I: Model Development, J. Am. Water Resour. As., 34, 73–89, 1998.

Bagnold, R. A.: Bedload transport in natural rivers, Water Resour. Res., 13, 303–312, 1977.

Beniston, M.: Mountain weather and climate: a general overview and a focus on climatic change in the Alps, Hydrobiologia, 562, 3–16, 2006.

Blake, W. H., Ficken, K. J., Taylor, P., Russell, M. A., and Walling, D. E.: Tracing crop-specific sediment sources in agricultural catchments, Geomorphology, 139–140, 322–329, 2012.

Brunetti, M., Maugeri, M., Nanni, T.,Auer, I., Bohm, R., and Schoner, W.: Precipitation variability and changes in the greater Alpine region over the 1800–2003 period, J. Geophys. Res.-Atmos., 111, D11107, doi:10.1029/2005JD006674, 2006.

Collins, A. L. and Walling, D. E.: Selecting fingerprint properties for discriminating potential suspended sediment sources in river basins, J. Hydrol., 261, 218–244, 2002.

Collins, A. L., Walling, D. E., and Leeks. G. J.: Source type ascription for fluvial suspended sediment based on a quantitative composite fingerprinting technique, Catena, 29, 1–27, 1997.

Collins, A. L., Walling, D. E., Stroud, R. W., Robson, M., and Peet, L. M.: Assessing damaged road verges as a suspended sediment source in the Hampshire Avon catchment, southern United Kingdom, Hydrol. Process., 24, 1106–1122, 2010.

Collins, A. L., Zhang, Y. S., Duethmann, D., Walling, D. E., and Black, K. S.: Using a novel tracing-tracking framework to source fine-grained sediment loss to watercourses at subcatchment scale, Hydrol. Process., 27, 959–974, 2013.

Evrard, O., Navratil, O., Ayrault, S., Ahmadi, M., Némery, J., Legout, C., Lefèvre, I., Poirel, A., Bonté, P., and Esteves, M.: Combining suspended sediment monitoring and fingerprinting to determine the spatial origin of fine sediment in a mountainous river catchment, Earth Surf. Proc. Land., 36, 1072–1089, 2011.

Flynn, K. F. and Van Liew, M. W.: Evaluation of SWAT for sediment prediction in a mountainous snowmelt-dominated catchment, T. ASABE, 54, 113–122, 2011.

Franks, S. W. and Rowan, J. S.: Multi-parameter fingerprinting of sediment sources: uncertainty estimation and tracer selection, in: Computational Methods in Water Resources XIII, edited by: Bentley, L. R., Balkema, Rotterdam, 1067–1074, 2000.

Fuhrer, J., Beniston, M., Fischlin, A., Frei, C., Goyette, S., Jasper, K., and Pfister, C.: Climate risks and their impact on agriculture and forests in Switzerland, Climatic Change, 79, 79–102, 2006.

García-Ruiz, J. M. and El Barrio, G.: Effects geomorphologiques des activités humaines dans les milleux supraforestiers des Pyrénées espagnoles, Rev. géograph. Pyrénées et du Sud-Ouest, 61, 255–270, 1990.

García-Ruiz, J. M., Puigdefábregas, J., and Creus, J.: Los Recursos Hídricos Superficiales del Alto Aragón, Instituto de Estudios Altoaragoneses, Huesca, 1985.

Garcia-Ruiz, J. M., Lasanta, T., Ruiz-Flano, P., Ortigosa, L., White, S., Gonzalez, C., and Marti, C.: Land-use changes and sustainable development in mountain areas: a case study in the Spanish Pyrenees, Landscape Ecol., 11, 267–277, 1996.

García-Ruiz, J. M., Beguería, S., López-Moreno, J. I., Lorente, A., and Seeger, M.: Los Recursos Hídricos Superficiales del Pirineo Aragonés y su Evolución Reciente, Geoforma Ediciones, Logroño, Spain, 2001.

Gellrich, M. and Zimmermann, N. E.: Investigating the regional-scale pattern of agricultural land abandonment in the Swiss Mountains: a spatial statistical modelling approach, Landscape Urban Plan., 79, 65–76, 2007.

Giannecchini, R., Naldini, G., D'Amato Avanzi, G., and Puccinelli, A.: Modelling of the initiation of rainfall-induced debris flows in the Cardoso basin (Apuan Alps, Italy), Quatern. Int., 171–172, 108–117, 2007.

Gikas, G. D., Yiannakopoulou, T., and Tsihrintzis, V. A.: Modeling of non-point source pollution in a Mediterranean drainage basin, Environ. Model Assess., 11, 219–233, 2006.

Granger, S. J., Bol, R., Butler, P. J., Haygarth, P. M., Naden, P., Old, G., Owens, P. N., and Smith, B. P. G.: Processes affecting transfer of sediment and colloids, with associated phosphorus, from intensively farmed grasslands: tracing sediment and organic matter, Hydrol. Process., 21, 417–422, 2007.

Heinemann, H. G.: A new sediment trap efficiency curve for small reservoirs, Water Resour. Bull., 17, 825–830, 1981.

Höchtl, F., Lehringer, S., and Konold, W.: "Wilderness" what it means when it becomes a reality – a case study from the southwestern Alps, Landscape Urban Plan., 70, 85–95, 2005.

Horton, P., Schaefli, A., Mezghani, B., Hingray, B., and Musy, A.: Assessment of climate-change impacts on alpine discharge regimes with climatemodel uncertainty, Hydrol. Process., 20, 2091–2109, 2006.

Jasper, K., Calanca, P., Gyalistras, D., and Fuhrer, J.: Differential impacts of climate change on the hydrology of two alpine river basins, Climate Res., 26, 113–129, 2004.

Koiter, A. J., Owens, P. N., Petticrew, E. L., and Lobb, D. A.: The behavioural characteristics of sediment properties and their implications for sediment fingerprinting as an approach for identifying sediment sources in river basins, Earth-Sci. Rev., 125, 24–42, 2013.

Lasanta, T., Gonzaléz-Hildalgo, J. C., Vicente-Serrano, S. M., and Sferi, E.: Using landscape ecology to evaluate an alternative management scenario in abandoned Mediterranean mountain areas, Landscape Urban Plan., 78, 110–114, 2006.

López-Moreno, J. I., Beguería, S., and García-Ruiz, J. M.: El régimen del río Ésera, Pirineo Aragonés, y su tendencia reciente, Bol. Glaciol. Aragon., 3, 131–162, 2002.

Martínez-Carreras, N., Udelhoven, T., Krein, A., Gallart, F., Iffly, J. F., Ziebel, J., Hoffmann, L., Pfister, L., and Walling, D. E.: The use of sediment colour measured by diffuse reflectance spectrometry to determine sediment sources: application to the Attert River catchment (Luxembourg), J. Hydrol., 382, 49–63, 2010a.

Martínez-Carreras, N., Krein, A., Gallart, F., Iffly, J. F., Pfister, L., Hoffmann, L., and Owens, P. N.: Assessment of different colour parameters for discriminating potential suspended sediment sources and provenance: a multi-scale study in Luxembourg, Geomorphology, 118, 118–129, 2010b.

Meusburger, K. and Alewell, C.: Impacts of anthropogenic and environmental factors on the occurrence of shallow landslides in an alpine catchment (Urseren Valley, Switzerland), Nat. Hazards Earth Syst. Sci., 8, 509–520, doi:10.5194/nhess-8-509-2008, 2008.

Motha, J. A., Wallbrink, P. J., Hairsine, P. B., and Grayson, R. B.: Determining the sources of suspended sediment in a forested catchment in southeastern Australia, Water Resour. Res., 39, 1059, doi:doi:10.1029/2001WR000794, 2003.

Nash, J. E. and Sutcliffe, J. V.: River flow forecasting through conceptual models: I. A discussion of principles, J. Hydrol., 10, 282–290, 1970.

Navas, A. and Machín, J.: Spatial distribution of heavy metals and arsenic in soils of Aragón (northeast Spain): controlling factors and environmental implications, Appl. Geochem., 17, 961–973, 2002.

Navas, A., Soto, J., and López-Martínez, J.: Radionuclides in soils of Byers Peninsula, South Shetland Islands, Western Antarctica, Appl. Radiat. Isotopes, 62, 809–816, 2005a.

Navas, A., Soto, J., and Machín, J.: Mobility of natural radionuclides and selected major and trace elements along a soil toposequence in the central Spanish Pyrenees, Soil Sci., 170, 743–757, 2005b.

Neitsch, S. L., Arnold, J. G., Kiniry, J. R., Srinivasan, R., and Williams, J. R.: Soil and Water Assessment Tool Input/output fifi le documentation: Version 2009, USDA, Soil and Water Research/Blackland Research Center, Texas, 2010.

Owens, P. N., Walling, D. E., and Leeks, G. J. L.: Tracing fluvial suspended sediment sources in the catchment of the River Tweed, Scotland, using composite fingerprints and a numerical mixing model, in: Tracers in Geomorphology, edited by: Foster, I. D. L., John Wiley and Sons Ltd., Chichester, 291–308, 2000.

Palazón, L. and Navas, A.: Sediment production of an alpine catchment with SWAT, Z. Geomorphol., 57, 69–85, 2013.

Puigdefábregas, J. and Creus, J.: Pautas espaciales de la variación climática en el Alto Aragón., Publ. Centro Pirenaico de Biol. Exp., 7, 23–34, 1973.

Rahman, K., Maringanti, C., Beniston, M., Widmer, F., Abbaspour, K., and Lehman, A.: Streamflow modeling in a highly managed mountainous glacier watershed using SWAT: the Upper Rhone River watershed case in Switzerland, Water Resour. Manage., 27, 323–339, 2013.

Rostamian, R., Jaleh, A., Afyuni, M., Mousavi, S. F., Heidarpour, M., Jalalian, A., and Abbaspour, K. C.: Application of a SWAT model for estimating runoff and sediment in two mountainous basins in central Iran, Hydrolog. Sci. J., 53, 977–988, 2008.

Schindler Wildhaber, Y., Bänninger, D., Burri, K., and Alewell, C.: Evaluation and application of a portable rainfall simulator on subalpine grassland, Catena, 91, 56–62, 2012.

Schmidli, J. and Frei, C.: Trends of heavy precipitation and wet and dry spells in Switzerland during the 20 century, Int. J. Climatol., 25, 753–771, 2005.

Smith, H. G. and Blake, W. H.: Sediment fingerprinting in agricultural catchments: a critical reexamination of source discrimination and data corrections, Geomorphology, 204, 177–191, 2014.

Stanchi, S., Freppaz, M., and Zanini, E.: The influence of Alpine soil properties on shallow movement hazards, investigated through factor analysis, Nat. Hazards Earth Syst. Sci., 12, 1845–1854, doi:10.5194/nhess-12-1845-2012, 2012.

Van Cleef, D. J.: Determination of ^{226}Ra in soil using ^{214}Pb and ^{214}Bi inmediately after sampling, Health Phys., 67, 288–289, 1994.

Walden, J., Slattery, M. C., and Burt, T. P.: Use of mineral magnetic measurements to fingerprint suspended sediment sources: approaches and techniques for data analysis, J. Hydrol., 202, 353–372, 1997.

Walling, D. E.: The evolution of sediment source fingerprinting investigations in fluvial systems, J. Soil Sediment, 13, 1658–1675, 2013.

Wilkinson, S. N., Hancock, G. J., Bartley, R., Hawdon, A. A., and Keen, R. J.: Using sediment tracing to assess processes and spatial patterns of erosion in grazed rangelands, Burdekin River basin, Australia, Agr. Ecosyst. Environ., 180, 90–102, 2012.

Williams, J. R.: Sediment-yield prediction with universal equation using runoff energy factor, in: Present and prospective technology for predicting sediment yield and sources, in: Proceedings of the Sediment-Yield Workshop, USDA sediment Lab, Oxford, 244–252, 1975.

Williams, J. R. and Berndt, H. D.: Sediment yield prediction based on watershed hydrology, Transact. Amer. Soc. Agricult. Biol. Engin., 20, 1100–1104, 1977.

Yu, L. and Oldfield, F.: A multivariate mixing model for identifying sediment source from magnetic measurements, Quaternary Res., 32, 168–181, 1989.

Yu, M., Chen, X., Li, L., Bao, A., and de la Paix, M. J.: Streamflow simulation by SWAT using different precipitation sources in large arid basins with scarce raingages, Water Resour. Manag., 25, 2669–2681, 2011.

Zhang, X., Srinivasan, R., Debele, B., and Hao, F.: Runoff simulation of the headwaters of the Yellow River using the SWAT model with three snowmelt algorithms, J. Am. Water Resour. As., 44, 48–61, 2008.

Table 1. Distribution of land covers, soil types and slope ranges (%) in SWAT input data of the Benasque catchment (BC) and of subcatchments (PNS: Paso Nuevo; and LS: Linsoles subcatchments).

	Type	Area (%)		
		BC	PNS	LS
Land covers	Urban	0.1	0.0	0.2
	Alluvial deposits	0.3	0.0	0.4
	Pine forests	17.7	17.4	17.9
	Mixed forests	2.6	1.3	3.3
	Deciduous forests	5.3	1.2	7.5
	Evergreen forests	6.9	12.3	4.0
	Scrublands	2.4	0.8	3.3
	Disperse scrublands	16.5	19.0	15.2
	Pastures	16.3	10.2	19.6
	Range grasses	3.8	0.8	5.5
	Rock outcrops	27.6	36.4	22.9
	Water	0.4	0.6	0.2
Soil types	Cambisols	22.7	28.1	19.8
	Fluvisols	0.7	0.2	1.0
	Kastanozems	29.5	21.7	33.7
	Leptosols	13.7	13.6	13.8
	Phaeozems	5.7	0.0	8.8
	Rock outcrop	27.6	36.4	22.9
Slope ranges	0–20	7.9	5.8	9.0
	20–40	20.9	17.3	22.7
	40–60	27.9	27.4	28.2
	60–75	17.4	18.2	17.0
	75–9999	25.9	31.2	23.1

Table 2. Soil specific sediment yields (SSY; $\mathrm{t\,ha^{-1}\,year^{-1}}$) simulated by SWAT for the period 2003–2006.

	Period	2003	2004	2005	2006
Cambisols	1.56	3.73	0.44	0.68	1.41
Fluvisols	0.16	0.46	0.01	0.02	0.15
Kastanozems	0.57	1.49	0.08	0.04	0.68
Leptosols	0.55	1.58	0.45	0.04	0.12
Phaeozems	0.10	0.28	0.02	0.02	0.07

Title Page
Abstract | Introduction
Conclusions | References
Tables | Figures
◀◀ | ▶▶
◀ | ▶
Back | Close
Full Screen / Esc
Printer-friendly Version
Interactive Discussion

Table 3. Statistics measures of the tracer properties for the potential sediment sources (KSPH: Kastanozems/Phaeozems; FL: Fluvisols; CM: Cambisols; and CbS: channel bed sediments) (Units: Textural classes: %; Radionuclide: $\mathrm{Bq\,kg^{-1}}$; low frequency mass specific magnetic susceptibility $10^{-8}\,\mathrm{m^3\,kg^{-1}}$ and magnetic susceptibility frequency dependence %; total elemental composition: $\mathrm{mg\,kg^{-1}}$).

	KSPH	$n = 3$			FL	$n = 3$			CM	$n = 2$			CbS	$n = 3$		
	m	dv	min	max	m	dv	min	max	m	dv	min	max	m	dv	min	max
Sand	11.2	4.3	6.2	14.1	27.5	7.0	20	33.8	16.45	0.92	15.8	17.1	21.3	16.9	1.9	32.2
Silt	71.7	1.5	70.3	73.2	65.7	6.0	60	72.0	72.75	2.19	71.2	74.3	69.4	8.9	62.4	79.5
Clay	17.2	3.0	15.3	20.6	6.9	1.0	6.25	8.0	10.825	3.08	8.65	13	9.2	8.2	3.7	18.6
^{40}K	712.3	26.4	682	730	773.0	30.3	749	807.0	699.5	34.65	675	724	740.7	97.5	666	851
^{137}Cs	136.2	66.2	79.5	209	62.0	10.7	50.9	72.3	61.4	17.96	48.7	74.1	5.9	6.0	0	11.9
^{210}Pb$_{ex}$	258.0	159.4	163.8	442	264.1	81.6	180.9	343.9	145.35	31.04	123.4	167.3	37.0	40.9	0	80.9
^{226}Ra	38.0	4.4	33	41.2	58.2	6.6	51.1	64.1	50.65	5.73	46.6	54.7	75.7	25.8	46.3	94.1
^{232}Th	75.3	14.1	59.9	87.7	84.9	8.8	78.7	94.9	60.2	16.12	48.8	71.6	77.2	7.3	72.6	85.6
^{238}U	53.0	4.9	49.3	58.5	218.7	71.4	139	277.0	162.4	135.20	66.8	258	100.4	35.2	63.1	133
SOC	12.7	3.9	9.43	17	4.0	1.0	2.93	4.9	9.91475	1.26	9.0215	10.808	0.8	0.6	0.326	1.46
LF	108.6	62.2	38.3	156.6	25.0	1.9	23.7	27.2	43.6	46.81	10.5	76.7	24.6	22.3	11.2	50.3
FD	8.9	2.9	5.48	10.54	3.7	2.6	1.69	6.6	5.21	3.32	2.86	7.56	4.5	2.6	1.59	6.5
Al	51 140.0	5389.7	44 970	54 930	59 326.7	4787.0	54 860	64 380.0	42 220	8103.44	36 490	47 950	55 326.7	4989.8	50 100	60 040
As	102.3	61.8	41.89	165.4	31.9	3.7	28.3	35.6	28.73	3.15	26.5	30.96	31.4	13.3	17.8	44.36
Be	2.1	0.2	1.88	2.34	2.6	0.5	2	3.0	1.61	0.00	1.61	1.61	2.1	0.3	1.77	2.4
Bi	30.8	3.8	26.44	33.15	34.4	3.7	30.58	37.9	32.125	4.02	29.28	34.97	41.6	7.1	35.75	49.56
B	1873.3	348.5	1500	2190	2240.0	170.9	2060	2400.0	2725	516.19	2360	3090	2693.3	664.3	1930	3140
Ca	5002.7	4103.7	2312	9726	21 356.7	4270.8	17 350	25 850.0	8532	5922.73	4344	12 720	31 810.7	19 564.3	9612	46 540
Cd	0.6	0.1	0.53	0.76	1.0	0.2	0.82	1.2	0.675	0.06	0.63	0.72	0.9	0.5	bdl	1.28
Co	0.4	0.0	bdl	bdl	18.0	15.3	bdl	28.2	8.265	2.81	6.28	10.25	8.1	2.6	5.47	10.61
Cr	100.2	10.4	90.48	111.2	79.0	12.5	71.26	93.5	59.23	2.40	57.53	60.93	79.6	13.2	64.83	90.03
Cu	24.3	7.5	16.07	30.55	29.9	4.8	24.51	33.9	21.275	0.26	21.09	21.46	36.4	9.9	25.03	42.53
Fe	48 646.7	8073.5	39 920	55 850	47 980.0	5508.9	43 830	54 230.0	41 715	9397.45	35 070	48 360	54 090.0	12 384.6	44 390	68 040
K	14 146.7	993.2	13 000	14 740	14 710.0	1022.4	13 530	15 330.0	9969.5	1429.06	8959	10 980	14 116.7	584.0	13 680	14 780
Li	69.9	3.3	67.18	73.57	73.1	25.8	50.89	101.4	68.675	21.96	53.15	84.2	79.9	14.9	63.51	92.53
Mg	2735.9	2951.1	897.8	6140	7791.0	1674.9	6594	9705.0	3829	1137.03	3025	4633	3864.3	2279.9	1232	5214
Mn	975.2	460.7	653.4	1503	707.4	71.3	634.2	776.7	634.45	513.43	271.4	997.5	428.5	45.3	389.5	478.2
Mo	1.4	0.5	1	1.9	1.6	0.4	1.19	1.9	1.77	0.11	1.69	1.85	4.4	2.8	1.16	6.46
Na	7124.0	926.1	6279	8114	7778.3	585.7	7114	8220.0	5886.5	734.68	5367	6406	6343.0	321.5	6102	6708
Ni	39.0	8.3	31.24	47.69	47.0	10.3	38.18	58.3	30.01	6.34	25.53	34.49	46.5	6.7	38.71	50.8
Pb	34.9	7.0	26.85	39.76	69.8	20.9	45.84	84.7	104.975	92.67	39.45	170.5	38.5	4.7	33.16	41.74
P	1161.3	124.9	1023	1266	1286.0	172.0	1088	1399.0	1704	888.13	1076	2332	979.8	143.7	846.5	1132
Sb	11.7	4.4	7.72	16.36	3.3	0.8	2.79	4.1	2.065	0.83	1.48	2.65	3.7	1.0	2.62	4.34
Se	1.4	0.9	0.4	2.26	1.6	0.7	1.07	2.4	1.685	0.42	1.39	1.98	1.4	1.0	0.4	2.43
S	705.7	147.5	539.3	820.2	912.9	82.4	846.2	1005.0	805.95	74.60	753.2	858.7	1776.8	1369.3	920.3	3356
Sr	60.0	19.2	47.63	82.1	158.7	16.7	144.7	177.1	74.675	47.84	40.85	108.5	151.0	73.4	69.93	213
Ti	5723.3	714.5	5170	6530	5336.7	250.1	5090	5590.0	5235	530.33	4860	5610	4870.0	729.2	4400	5710
Tl	40.4	10.9	33.92	52.92	57.3	5.1	51.88	62.1	45.265	11.87	36.87	53.66	49.4	13.4	34.74	60.89
V	124.8	13.9	115.4	140.8	118.9	25.8	94.73	146.0	111.25	5.87	107.1	115.4	152.3	20.7	137.5	175.9
Zn	102.9	34.6	80.59	142.7	243.7	75.5	157.4	297.9	300.3	148.35	195.4	405.2	111.3	17.0	94.6	128.5

m: mean; dv: deviation standart; min: minimum; max: mximum; SOC: soil organic carbon; LF: low frequency mass specific magnetic susceptibility; FD: magnetic susceptibility frequency dependence

Title Page
Abstract Introduction
Conclusions References
Tables Figures
◂◂ ▸▸
◂ ▸
Back Close
Full Screen / Esc
Printer-friendly Version
Interactive Discussion

Table 4. Results of the stepwise discriminant function analysis to identify the optimum composite fingerprint for the assessed fingerprinting options.

Fingerprinting options	Fingerprint property added	Wilk's lambda	Significance
Soil and channel bed sources			
	^{137}Cs	0.2678	0.0206
	Zn	0.0802	0.0083
	^{238}U	0.0173	0.0027
Soil sources			
	K	0.1677	0.0115
	Sr	0.0228	0.0023
	^{238}U	0.001005	0.0003
	Sb	0.000065	0.0006
	LF	0.000001	0.0055

Table 5. Mean percentages of GOD and source contributions (standard deviations) from the multivariate mixing model for Kastanozems/Phaeozems (KSPH), Fluvisols (FL), channel bed sediments (CbS) and Cambisols (CM) sources to the Paso Nuevo and Linsoles reservoirs.

Fingerprinting options	Reservoirs	GOF	KSPH	FL	CbS	CM
Soil and channel bed sources	Paso Nuevo	80	0 (0)	83 (14)	0 (0)	16 (14)
	Linsoles	93	0 (0)	0 (0)	91 (1)	9 (1)
Soil sources	Paso Nuevo	83	7 (0)	87 (0)	–	6 (0)
	Linsoles	82	0 (0)	92 (0)	–	8 (0)

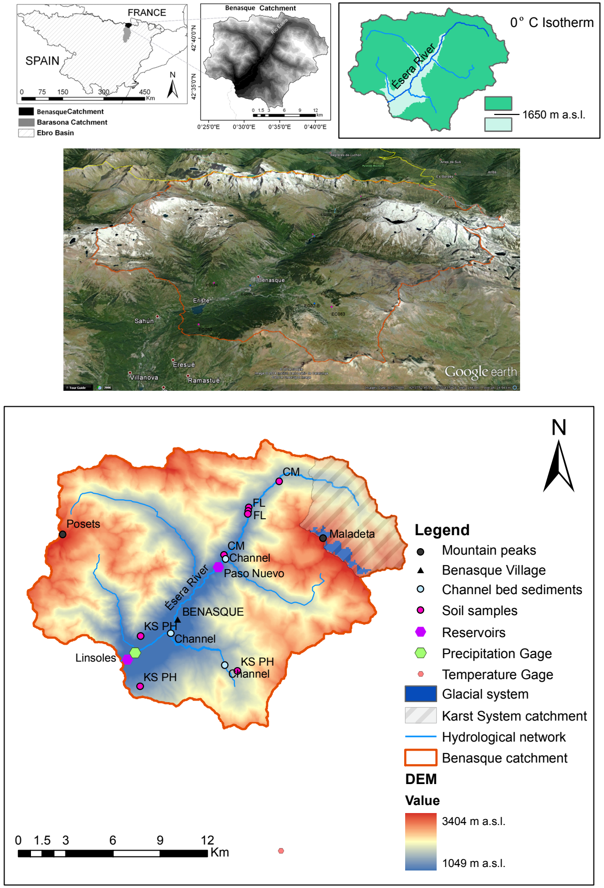

Fig. 1. Location of the Benasque catchment. Distribution of soil and sediment samples, the Paso Nuevo and Linsoles reservoirs and map of the 0 °C isotherm.

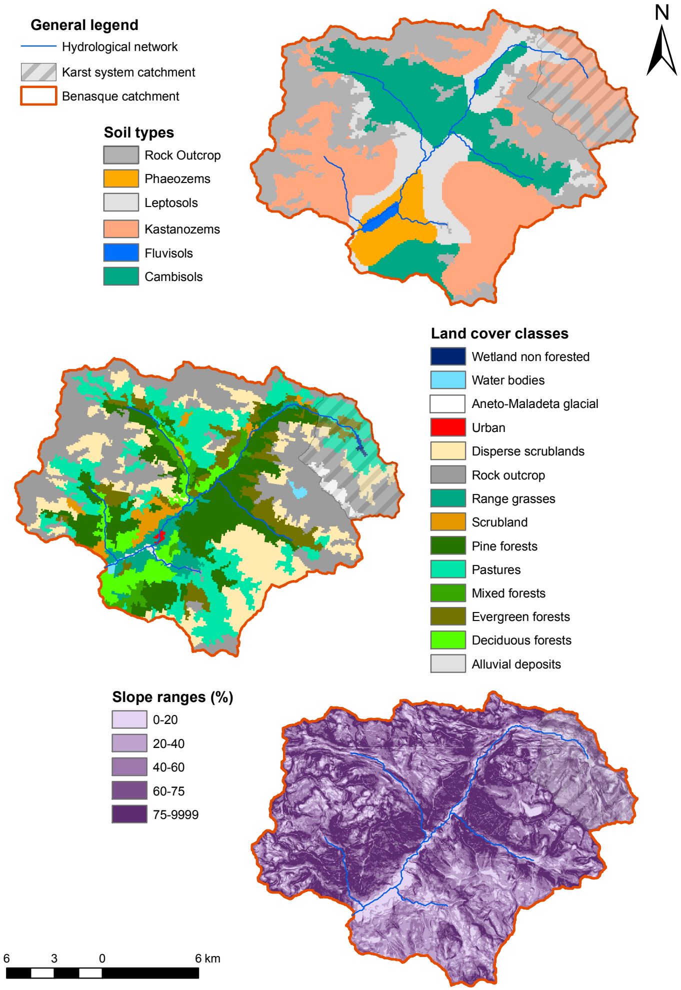

Fig. 2. Distribution of soil types, land covers and slopes ranges in the Benasque catchment.

Title Page
Abstract
Introduction
Conclusions
References
Tables
Figures
◀◀
▶▶
◀
▶
Back
Close
Full Screen / Esc
Printer-friendly Version
Interactive Discussion

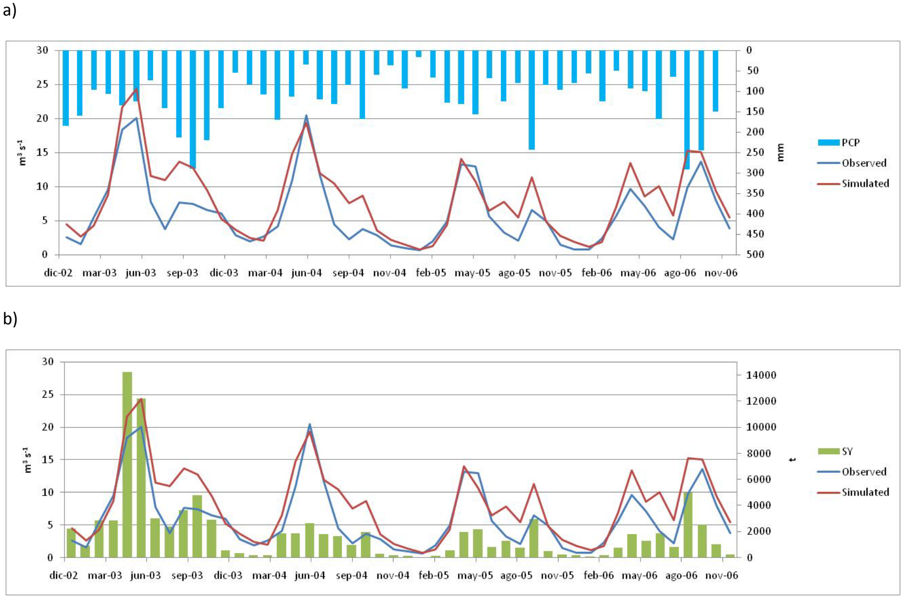

Fig. 3. Compared monthly hydrographs simulated by SWAT for the Linsoles reservoir inflow gauge station, with: **(a)** simulated monthly rainfall for the Benasque catchment and **(b)** simulated monthly sediment yields (SY; *t*).

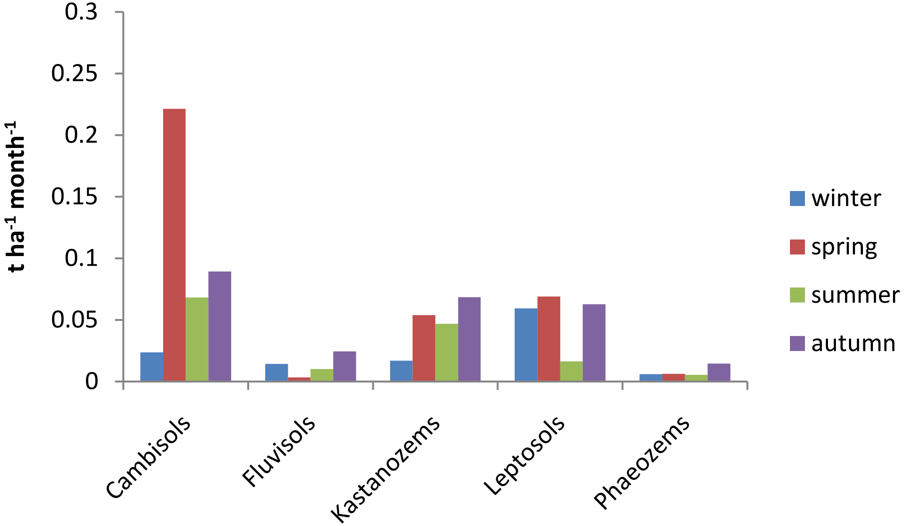

Fig. 4. Seasonal distribution of simulated soil specific sediment yield ($\mathrm{t\,ha^{-1}\ month^{-1}}$).